LARGE DIVALENT CATIONS AND ELECTROSTATIC POTENTIALS ADJACENT TO MEMBRANES

A Theoretical Calculation

STEVEN CARNIE
Department of Chemistry, State University of New York, Stony Brook, New York 11794

STUART MCLAUGHLIN
Department of Physiology and Biophysics, State University of New York, Stony Brook, New York 11794

ABSTRACT We have extended the Gouy-Chapman theory of the electrostatic diffuse double layer by considering the finite size of divalent cations in the aqueous phase adjacent to a charged surface. The divalent cations are modeled as either two point charges connected by an infinitely thin, rigid "rod" or two noninteracting point charges connected by an infinitely thin, flexible "string." We use the extended theory to predict the effects of a cation of length 10 Å (1 nm) on the zeta and surface potentials of phospholipid bilayer membranes. The predictions of the rod and string models are similar to one another but differ markedly from the predictions of the Gouy-Chapman theory. Specifically, the extended model predicts that a large divalent cation will have a smaller effect on the potential adjacent to a negatively charged bilayer membrane than a point divalent cation, that the magnitude of this discrepancy will decrease as the Debye length increases, and that a large divalent cation will produce a negative zeta potential on a membrane formed from zwitterionic lipids. These predictions agree qualitatively with the experimental results obtained with the large divalent cation hexamethonium. We discuss the biological relevance of our calculations in the context of the interaction of cationic drugs with receptor sites on cell membranes.

INTRODUCTION

The Gouy-Chapman-Stern theory, with its assumption that ions in the diffuse double layer are point charges, adequately describes the effects of alkaline earth cations on the electrostatic potential adjacent to phospholipid bilayer membranes (1, 2). The finite size of large divalent cations, such as the ganglionic blocker hexamethonium, however, cannot be ignored because the charges are separated by ~10 Å (1 nm), a distance comparable with the Debye length in a physiological, decimolar sodium chloride solution. Our objective is to describe theoretically the electrostatic potential adjacent to a membrane when the aqueous phase contains large divalent cations. Our analysis incorporates the finite size of the divalent cation into the Gouy-Chapman theory.

ANALYSIS

There are five major assumptions in the Gouy-Chapman theory: the electrical potential can be described by the combination of the Poisson and Boltzmann equations, the dielectric constant is uniform throughout the aqueous phase, the discrete charges at the interface may be replaced by a surface of uniform charge density, image charge effects are negligible, and the finite size of the ions in the aqueous phase may be ignored. These and other assumptions have been discussed in detail in various reviews (3–13). We modify only the last assumption. Specifically, we extend the Gouy-Chapman theory by considering a divalent cation to be either two point charges connected by a thin, rigid rod of length a or two charges connected by a thin, flexible string of length a. In the rod model we ignore any interactions between the rods. In the string model we ignore intramolecular Coulomb interactions between the charges, interactions between strings, and interactions between the string and the surface. For simplicity, we assume that the aqueous solution contains a single species of a monovalent cation, a monovalent anion, and a large divalent cation. The monovalent ions are represented by point charges. We also assume that none of the ions adsorb to the phospholipids comprising the membrane; the validity of this assumption is discussed in the accompanying paper (14). The Poisson equation for a one dimensional system is, in SI units,

$$\frac{d^2\psi(x)}{dx^2} = -(1/\epsilon_r\epsilon_o)\sum_i q_i\rho_i(x), \quad (1)$$

where $\psi(x)$ is the mean electrostatic potential in the aqueous diffuse double layer a distance x from the surface located at $x = 0$, q_i is the charge of each species, $\rho_i(x)$ is the mean number density of ions of species i at a distance x from the surface, ϵ_r is the dielectric constant, and ϵ_o is the permittivity of free space. We label the two charges on the divalent cation as A and B. By symmetry the local density of A will equal that of B, $\rho_A(x)$

Dr. Carnie's present address is the Department of Chemistry, University of Toronto, Lash Miller Chemical Laboratories, 80 St. George Street, Toronto, Ontario M5S 1A1, Canada.

$= \rho_B(x)$. For our system the summation on the right-hand side of Eq. 1 then becomes

$$\sum_i q_i\rho_i(x) = e[\rho_M(x) - \rho_X(x) + 2\rho_A(x)], \quad (2)$$

where e is the magnitude of the electronic charge, M represents a monovalent cation, and X a monovalent anion. Integrating Eq. 1 once, using the boundary conditions that $d\psi/dx \to 0$ as $x \to \infty$, we obtain

$$\frac{d\psi(x)}{dx} = (1/\epsilon_r\epsilon_o)\int_x^\infty dy \sum_i q_i\rho_i(y). \quad (3)$$

Using the boundary conditions that $\psi(x)$ and $x[d\psi(x)/dx] \to 0$ as $x \to \infty$ and integrating by parts, we obtain the identity

$$\psi(x) = x\frac{d\psi(x)}{dx} + \int_x^\infty dy(y)\frac{d^2\psi(y)}{dy^2}. \quad (4)$$

Substituting Eqs. 1 and 3 into Eq. 4 yields

$$\psi(x) = (1/\epsilon_r\epsilon_o)\int_x^\infty dy(x - y)\sum_i q_i\rho_i(y). \quad (5)$$

Eq. 5 is solved numerically, subject to the following boundary condition

$$\sigma = -\int_0^\infty dy \sum_i q_i\rho_i(y) = -\epsilon_r\epsilon_o \left.\frac{d\psi}{dx}\right|_{x=0}. \quad (6)$$

Eq. 6 states that the surface charge, σ, must be balanced by the net charge in the aqueous diffuse double layer for the condition of electroneutrality to be satisfied. The Boltzmann equation predicts that

$$\rho_M(x) = \rho_M \exp[-\beta e\psi(x)] \quad (7)$$

$$\rho_X(x) = \rho_X \exp[\beta e\psi(x)], \quad (8)$$

where $\beta = 1/kT$, T is the absolute temperature, k is the Boltzmann constant, $\rho_M = \rho_M(\infty)$, and $\rho_X = \rho_X(\infty)$. In the Appendix we derive the following expression for $\rho_A(x)$

$$\rho_A(x) = \rho_D\{\exp[-\beta e\psi(x)]\}\langle \exp[-\beta e\psi(z)]\rangle, \quad (9)$$

where $\rho_D = \rho_A(\infty)$ is the mean number density of divalent ions, D, in the bulk aqueous phase. Eq. 9 has the following simple interpretation. $\rho_A(x)/\rho_D$, which is the probability of finding a given end of the divalent cation at a position x normalized to the probability of finding it at $x = \infty$, is simply $\exp[-\beta e\psi(x)]$ weighted by the configurations of the other end of the molecule. When $x > a$, the length of either the rod or the string, the weighting is obtained by integrating over either the surface of a sphere of radius a for the rod model or the volume of a sphere of radius a for the string model. Specifically, in the rod model the weighting is given by the spatial average, $[1/(2a)]\int_{x-a}^{x+a} dz = \langle\ \rangle$, of the probability the other end of the molecule is a distance z from the surface, which is $\exp[-\beta e\psi(z)]$. In the string model the weighting is given by the spatial average, $[3/(4a^3)]\int_{x-a}^{x+a} dz\,(a^2 - z^2) = \langle\ \rangle$, of $\exp[-\beta e\psi(z)]$. When $x < a$ the weighting is subject to the restriction that the other end of the molecule cannot penetrate the interface, and Eq. 9 becomes, in general,

$$\rho_A(x) = \rho_D\{\exp[-\beta e\psi(x)]\} \cdot \{[1/(2a)]\int_{\max[0,\,x-a]}^{x+a} dz \exp[-\beta e\psi(z)]\} \quad (10)$$

in the rod model and

$$\rho_A(x) = \rho_D\{\exp[-\beta e\psi(x)]\} \{[3/(4a^3)]\int_{\max[0,\,x-a]}^{x+a} dz(a^2 - z^2)\exp[-\beta e\psi(z)]\} \quad (11)$$

in the string model. The combination of Eqs. 5, 7, 8, and either Eq. 10 or 11, subject to the electroneutrality boundary condition, is an integral equation in one variable, $\psi(x)$, which is solved numerically following the method of Carnie et al. (15).

RESULTS

In this section we present the results of a numerical analysis of Eqs. 5–11. We determine the profiles of the electrostatic potential adjacent to membranes with different surface charge densities, varying the concentrations of monovalent and divalent cations in the aqueous phase. We assume that the temperature is 25°C and that the length of the divalent cation, a, is 10 Å (1 nm) in all calculations. Once this length is set, the theory contains no adjustable parameters.

The set of Eqs. 5–11 can be rewritten in differential form to obtain a second-order nonlinear differential equation with advanced and retarded arguments for $\psi(x)$. It is not easy to solve such equations. When written in integral form, however, Eqs. 5–11 are similar in structure to the integral equations used in a double-layer theory where the ions were modeled as charged hard spheres. Carnie et al. (15) developed numerical methods to solve such equations, and we use a similar, straightforward numerical method to solve Eqs. 5–11. The concentration and potential profiles are represented by their values at regular intervals on the positive x axis, the integrals calculated by Simpson's rule and the equations solved by iteration (15). The electroneutrality condition is enforced by rescaling the diffuse dou-

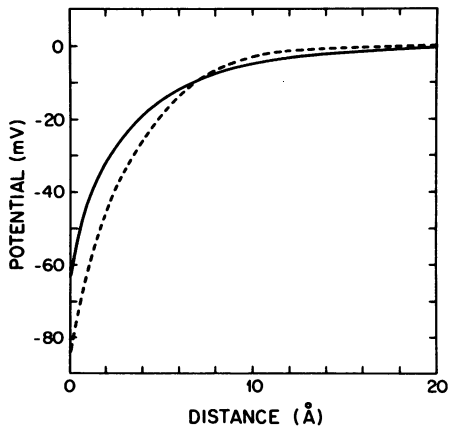

FIGURE 1 The electrostatic potential predicted by the Gouy-Chapman (solid curve, —) and rod (dashed curve, ---) models, plotted as a function of the distance from the membrane. The concentrations of both the monovalent and divalent cations are assumed to be 0.1 M, and the charge density, σ, is assumed to be $-1/70$ Å^2 ($-1/0.7$ nm^2). Note that the potential decays more rapidly in the rod than in the Gouy-Chapman model.

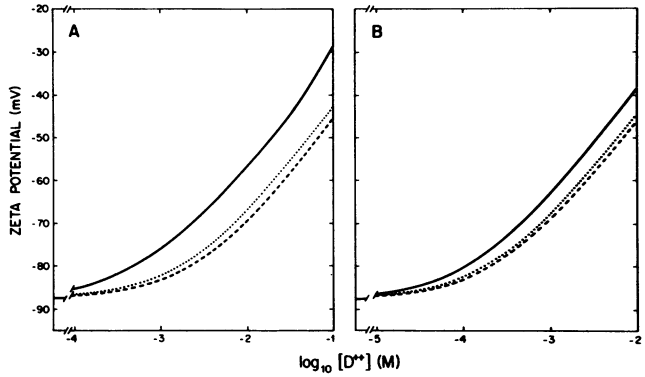

FIGURE 2 The predicted value of the zeta potential, the electrostatic potential a distance 2 Å (0.2 nm) from the surface of a bilayer membrane, plotted as a function of the concentration of divalent cation in the aqueous phase, $[D^{++}]$. The predictions of the Gouy-Chapman model are illustrated by the solid curves (—), the predictions of the string model by the dotted curves (···), and the predictions of the rod model by the dashed curves (---). (*A*) $\sigma = -1/70$ Å^2 ($-1/0.7$ nm^2), $[M^+] = 0.1$ M. (*B*) $\sigma = -1/420$ Å^2 ($-1/4.2$ nm^2), $[M^+] = 0.01$ M.

ble-layer charge resulting from each iteration step before using it as an input for the next step.[1] The decay of the potential is illustrated in Fig. 1 for the rod (dashed curve) and the Gouy-Chapman (solid curve) models. An important feature of the numerical method is the analytical incorporation of the correct long-range behavior of the potential and concentration profiles. Specifically, we note that the decay length for the rod model differs from the value given by the Gouy-Chapman theory. Failure to include this deviation leads to a violation of the electroneutrality condition.[2]

We intend to compare the theoretical predictions of the Gouy-Chapman, rod, and string models with the experimental zeta potential and surface potential measurements presented in the accompanying paper (14). The surface potential cannot be measured directly but the zeta potential, the electrostatic potential at the hydrodynamic plane of shear, can be determined experimentally from electrokinetic mobility measurements on vesicles. The available evidence (14, 17) indicates that the plane of shear is 2 Å (0.2 nm) from the surface of a phospholipid bilayer vesicle in a decimolar monovalent salt solution.[3] For this reason we illustrate the electrostatic potential 2 Å (0.2 nm) from the surface of the membrane predicted by the point (Gouy-Chapman), string, and rod models in Figs. 2 and 3. Fig. 2 *A* illustrates these predictions when the vesicle is formed from a negative lipid (e.g., phosphatidylserine) that has a surface area of 70 Å^2 (0.7 nm^2) and the monovalent salt concentration is 0.1 M. The predictions of the string (dotted curve) and rod (dashed curve) models differ significantly from the predictions of the Gouy-Chapman (solid curve) model: the finite size of the cation decreases its ability to screen the surface charges and reduce the magnitude of the potential. There is little difference between the predictions of the string and rod models; thus the flexibility of the molecules does not significantly affect their screening ability.

The results illustrated in Fig. 2 *A* may be compared with the results illustrated in Fig. 2 *B*, where the monova-

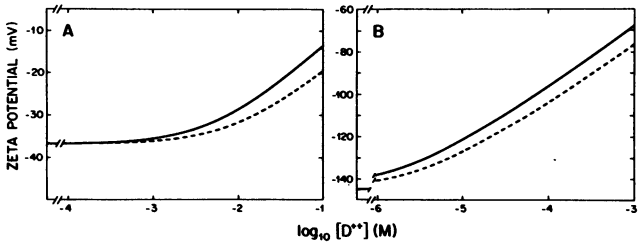

FIGURE 3 The predicted value of the zeta potential plotted as a function of the concentration of divalent cations in the aqueous phase, $[D^{++}]$. The predictions of the Gouy-Chapman model are illustrated by the solid curves (—) and the predictions of the rod model by the dashed curves (---). (*A*) $\sigma = -1/420$ Å^2 ($-1/4.2$ nm^2), $[M^+] = 0.1$ M. (*B*) $\sigma = -1/420$ Å^2 ($-1/4.2$ nm^2), $[M^+] = 0.001$ M.

[1]The usual mixing of iterates is also required. A mixing parameter equal to 0.5 is generally adequate (15, 16).

[2]To determine the actual decay length of the potential profile, we consider Eq. 5 for large values of x. Assuming that $\psi(x)$ decays exponentially, we can substitute Eqs. 2, 7, 8 and 10 into either Eq. 5 or Eq. 1 and linearize the exponential functions. This procedure is valid because the integral in Eq. 10 is of finite range. We obtain an equation that ensures consistency between the left and right-hand sides. For the rod model the actual decay length, $1/\kappa$, is given by the solution to the equation

$$\kappa^2 = \kappa_+^2\left[1 + 2R + R\frac{\sinh(\kappa a)}{\kappa a}\right], \qquad (12)$$

where κ_+ is the reciprocal of the Debye length in the case where there are no divalent cations in the solution, and R is the ratio of the divalent and monovalent cation concentrations. For the string model we obtain

$$\kappa^2 = \kappa_+^2\left\{1 + 2R + 3R\left[\frac{\cosh(\kappa a)}{(\kappa a)^2} - \frac{\sinh(\kappa a)}{(\kappa a)^3}\right]\right\}. \qquad (13)$$

Note that Eqs. 12 and 13 reduce to the Gouy-Chapman result, $\kappa^2 = \kappa_+^2(1 + 3R)$, when $a = 0$. The deviations due to the length of the divalent cation can be significant. For example, for 0.1 M monovalent salt and $R = 1$, κ exceeds $2\kappa_+$ by 14% in the rod model (Fig. 1).

[3]Recent results (1, 14, 18) indicate that the magnitude of the zeta potential of a phospholipid vesicle does not increase as much as predicted by the Gouy-Chapman-Stern theory when the concentration of monovalent salt is decreased from 0.1 to 0.01 and 0.001 M if one assumes that the plane of shear remains 2Å (0.2 nm) from the surface. If one assumes that the plane of shear shifts out to ~4 Å (0.4 nm) in a 0.01M and 10 Å (1 nm) in a 0.001 M monovalent salt solution, the theoretical predictions are consistent with the data. Neither this shift in the plane of shear nor the adsorption of monovalent ions to the membrane (17) are included in the rod and string models because these phenomena have no bearing on the main points we wish to make concerning the effect of size on the electrostatic behavior of divalent cations. For example, if one recalculates the quantities plotted in Fig. 2 *B* assuming that the plane of shear is 4 Å (0.4 nm) rather than 2 Å (0.2 nm) from the membrane, the resulting curves can be shifted to less negative values on the ordinate by 8.2 mV to produce agreement, within 2%, with the curves illustrated in Fig. 2 *B*.

lent salt concentration is reduced from 0.1 to 0.01 M. The magnitude of the charge density is also reduced, from $-1/70$ Å^2 ($-1/0.7$ nm^2) to $-1/420$ Å^2 ($-1/4.2$ nm^2), to maintain the zeta potential in the absence of divalent cations at -87 mV. The Gouy-Chapman, the string, and the rod models all predict that divalent cations screen the surface charge more effectively when the concentration of monovalent salt is decreased. The feature of Fig. 2 *B* we wish to stress, however, is that the predictions of the rod and string models agree more closely with the prediction of the Gouy-Chapman theory when the monovalent salt concentration is lower. For example, when the divalent cation concentration is 0.01 M, the Gouy-Chapman and the rod models predict zeta potentials that differ by 13 mV in 0.1 M and by 8 mV in 0.01 M monovalent salt. It is intuitively apparent why this is true: the Debye length increases from ~10 Å (1 nm) to 30 Å (3 nm) when the monovalent salt concentration decreases from 0.1 to 0.01 M, and the finite size of the divalent cations becomes less important when the Debye length increases.

Figs. 3 *A* and *B* illustrate the zeta potentials predicted by the Gouy-Chapman and the rod models when the membrane has a charge density of $-1/420$ Å^2 ($-1/4.2$ nm^2) and the monovalent salt concentrations are 0.1 and 0.001 M. The predictions of the string model, which are not illustrated, are very similar to the predictions of the rod model.

Figs. 4 and 5 are similar to Figs. 2 and 3, except the potential at the surface of the membrane, rather than the potential at a distance of 2 Å (0.2 nm) from the membrane, is graphed as a function of the log of the concentration of divalent cation. The qualitative features of the predicted zeta and surface potential curves are very similar. Specifically, the predictions of the Gouy-Chapman (solid curve) and rod (dashed curve) models differ significantly in 0.1 M

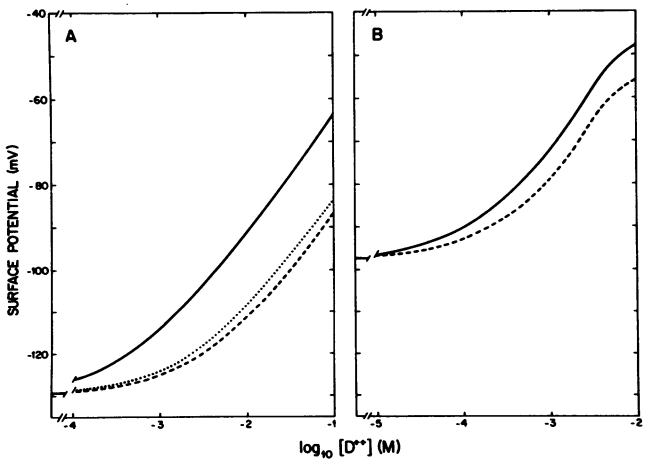

FIGURE 4 The surface potential plotted as a function of the concentration of divalent cation, $[D^{++}]$. The predictions of the Gouy-Chapman model are illustrated by the solid curves (—) and the predictions of the rod model by the dashed curves (---). (*A*) $\sigma = -1/70$ Å^2 ($-1/0.7$ nm^2), $[M^+] = 0.1$ M. (*B*) $\sigma = -1/420$ Å^2 ($-1/4.2$ nm^2), $[M^+] = 0.01$ M.

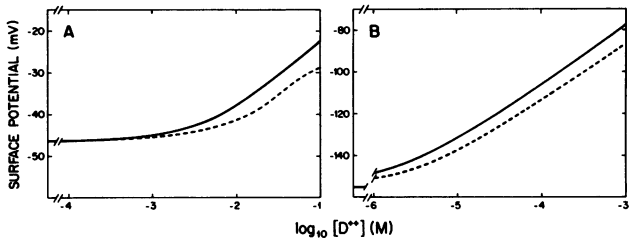

FIGURE 5 The surface potential plotted as a function of the concentration of divalent cation $[D^{++}]$. The predictions of the Gouy-Chapman model are illustrated by the solid curves (—), the predictions of the rod model by the dashed curves (---). (*A*) $\sigma = -1/420$ Å^2 ($-1/4.2$ nm^2), $[M^+] = 0.1$ M. (*B*) $\sigma = -1/420$ Å^2 ($-1/4.2$ nm^2), $[M^+] = 0.001$ M.

salt (Fig. 4 *A*). The flexibility of the molecules has little effect on the surface potential: the predictions of the rod (dashed curve) and string (dotted curve) models in Fig. 4 *A* are similar. When the monovalent salt concentration is reduced, the Debye length increases and the predictions of the Gouy-Chapman and rod models are in better agreement (Fig. 4 *B*).

The experimental zeta potential results, as well as the surface potential results from ^{31}P nuclear magnetic resonance (NMR) measurements on vesicles, compensation potential measurements on monolayers, and nonactin and gramicidin measurements on planar bilayer membranes, which are presented in the accompanying paper (14), are in accord with the theoretical predictions illustrated in Figs. 2–5. We can also use the extended theory to examine the effect of cations on the potential adjacent to bilayers formed from a phospholipid with zero net charge. The Gouy-Chapman theory predicts that addition of a nonadsorbing divalent cation will not change the zeta potential of a phospholipid vesicle formed from a zwitterionic lipid, such as phosphatidylcholine. The rod and string models, however, predict that the concentration of the divalent cation adjacent to the surface will be lower than in the bulk aqueous phase; this decrease in the concentration of cations leads to an excess of negative charges in the region adjacent to the membrane, which manifests itself as a negative zeta potential in electrokinetic measurements. Specifically, the rod model predicts that when 0.1 M of a large divalent cation (a = 10 Å [1 nm]) is added to a solution of vesicles formed from a zwitterionic lipid in a 0.1 M monovalent salt, the zeta and surface potentials should decrease from 0 to -2 mV.[4] The experimental results

[4]It is not possible to solve Eqs. 5–10 by the technique used here when the charge density on the membrane is zero. However, both the potential at the surface of the membrane and the potential 2 Å (0.2 nm) from the surface depend linearly on the charge density when the potential is small (<10 mV). By plotting the surface potential and the zeta potential as a function of the charge density and extrapolating the linear region of the curves to zero charge density, we conclude that both the zeta and surface potentials should be -2 mV when $[D^{++}] = [M^+] = 0.1$ M. In the Gouy-Chapman model the surface and zeta potentials are predicted to be zero when the charge density on the membrane is zero.

obtained with hexamethonium agree qualitatively with this theoretical prediction (14).

The biological activity of large divalent cations such as curare, hexamethonium, and decamethonium lies not with their screening ability but with their ability to adsorb to specific receptor sites such as the acetylcholine receptor in a muscle membrane. The ability of these drugs to adsorb to a receptor depends on the local concentration of the drug. The aqueous concentration of a large divalent cation at the surface of the membrane should be predicted more accurately by either the rod or the string model than by the Gouy-Chapman model. Fig. 6 illustrates the normalized probability, $\rho_A(x)/\rho_D$, of finding a given end of a large cation a distance x from a membrane formed from lipids that have no net charge when the bulk aqueous phase contains monovalent ions and only a trace concentration of the divalent cation. The Gouy-Chapman theory predicts that the surface and the bulk concentrations are identical (solid line). The rod and string models predict that for $x < a = 10$ Å (1 nm), the normalized probability decreases as x decreases, reaching a value of 0.5 at $x = 0$. We term this reduction in concentration near the membrane, which is due to the limitation on the integrals in Eqs. 10 and 11, "entropic repulsion."

The dashed line in Fig. 7 illustrates the normalized probability of finding a given end of a large divalent cation a distance x from the membrane when the membrane bears a negative charge. Note that when $x > a = 10$ Å (1 nm), the value of $\rho_A(x)/\rho_D$ predicted by the rod model is greater than the normalized probability of finding a point divalent cation at this distance, which is $\exp[-2\beta e\psi(x)]$ (solid line), i.e., the probability of finding a given end of a large divalent cation a distance x from the membrane is greater than the probability of finding a point divalent cation at this distance. This is because the other end of the large divalent cation can sample the energetically favorable region closer to the membrane than x (Eq. 9). Fig. 7 also illustrates that when $x < a = 10$ Å the entropic repulsion reduces the concentration of the divalent cation until, at $x = 8$ Å (0.8 nm) in this example, a crossover

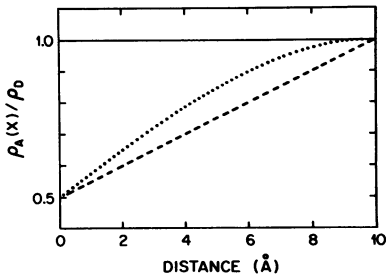

FIGURE 6 The probability of finding a given end of a large divalent cation a distance x from the membrane with no net charge, normalized to the probability of finding the molecule at $x = \infty$, plotted as a function of distance from the surface. The solid line (—) is the prediction of the Gouy-Chapman model. The dashed line (---) is the prediction of the rod model, and the dotted curve (· · ·) is the prediction of the string model.

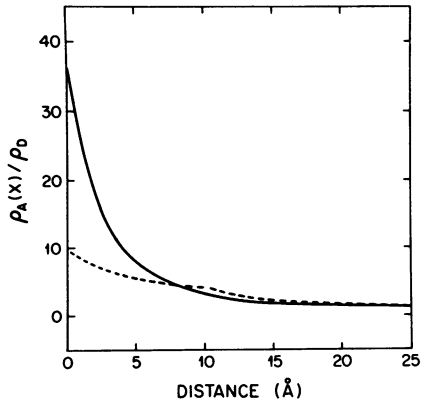

FIGURE 7 The probability of finding a given end of a large divalent cation a distance x from the membrane, normalized to the probability of finding the cation at $x = \infty$, plotted against the distance. The solid curve (—) is the prediction of the Gouy-Chapman model, and the dashed curve (---) is the prediction of the rod model. The concentration of divalent cation in the bulk aqueous solution is assumed to be sufficiently low that it does not affect the surface potential (Fig. 5 *A*). The charge density, σ, is assumed to be $-1/420$ Å^2 ($-1/4.2$ nm^2) and the monovalent salt concentration, [M$^+$], is assumed to be 0.1 M. The surface potential predicted by the Gouy equation is -46 mV.

occurs: $\langle \exp[-\beta e\psi(z)] \rangle = \exp[-\beta e\psi(x)]$ in Eq. 9, and the normalized probability of finding a given end of the molecule at $x = 8$ Å (0.8 nm) is equal to the normalized probability of finding a point divalent cation at this distance. When $x = 0$, the rod model predicts that $\rho_A(0)/\rho_D = \{\exp[-\beta e\psi(0)]\}\{[1/(2a)]\int_0^a dz\ \exp[-\beta e\psi(z)]\}$ (dashed line), which is less than $\exp[-2\beta e\psi(0)]$, the prediction of the Gouy-Chapman model (solid line). In the example illustrated in Fig. 7, the probability of finding a given end of a large divalent cation at $x = 0$ is a factor of 4 less than the probability of finding a point divalent cation at the origin.

The prediction of the string model is similar to the prediction of the rod model (results not shown). When $x > a = 10$ Å (1 nm), the string model predicts that the value of $\rho_A(x)/\rho_D$ lies between the values predicted by the rod and the Gouy-Chapman models. When $x < a = 10$ Å (1 nm), $\rho_A(x)/\rho_D$ is larger for the string than for the rod model. Specifically, the value of $\rho_A(x)/\rho_D$ predicted by the string model is ~20% larger than the value predicted by the rod model when $x < 5$ Å (0.5 nm). The values for $\rho_A(x)/\rho_D$ predicted by the string model form a smoother curve than the dashed curve in Fig. 7. This result is consistent with the results of Fig. 6, which illustrate that the entropic repulsion is less abrupt in the string than in the rod model.

DISCUSSION

We have extended the Gouy-Chapman theory by considering the finite size of the divalent cations in the diffuse double layer. The divalent cation is represented by two point charges joined by either rigid rods or flexible strings that do not occupy any volume and do not interact with

each other. These assumptions are obvious oversimplifications, as are several other assumptions common to the Gouy-Chapman theory (3–13) and our models. In spite of these theoretical limitations, the results of recent Monte Carlo computer experiments on a model of an electrical double layer indicate that the "the Gouy-Chapman theory as modified by Stern is found to work surprisingly well" (19). Bearing in mind the aphorism "if it works don't fix it," we note that four experimentally testable predictions emerge from our models. First, a large, nonadsorbing divalent cation should have a smaller effect on the zeta and surface potentials of negatively charged bilayer membranes than a hypothetical point divalent cation. Second, the discrepancy between the experimentally observed effects of the large divalent cation and the theoretical predictions of the Gouy-Chapman model should decrease as the monovalent salt concentration decreases. Third, a large divalent cation should produce a negative zeta potential on membranes formed from zwitterionic lipids. Fourth, as the size of a nonadsorbing divalent cation is reduced, the experimental results should agree more closely with the predictions of the Gouy-Chapman theory. The experiments described in the accompanying paper (14) are consistent with these four predictions.

The calculations presented here suggest that the finite size of many biologically active divalent cations, e.g., decamethonium, hexamethonium, saxitoxin, and curare, plays an important role in their interactions with receptors on membranes. Consider, for example, the elegant study of Henderson et al. (20) of the effect of calcium on the apparent binding constants of monvalent and divalent toxins with the sodium channel. If it is assumed that tetrodotoxin, (TTX), a monovalent cation, and saxitoxin (STX), a divalent cation, are point charges, then the Boltzmann equation can be used to relate the apparent binding constants to the intrinsic binding constants of these molecules. Henderson et al. (20) calculated the change produced by calcium in the surface potential adjacent to the sodium channel in nerve membranes by measuring the change in the ratio of the apparent binding constants of TTX and STX upon addition of calcium. There is also evidence for the existence of negative charges adjacent to or on the acetylcholine receptor is muscle membranes (21–23). Van der Kloot and Cohen (24) compared the literature values for the relative affinities of acetylcholine and curare with the acetylcholine receptor. They treated acetylcholine, a monovalent cation, and curare, a divalent cation, as point charges and used the Boltzmann equation to calculate changes in the surface potential when the concentration of inorganic ions was changed. They applied the Gouy-Chapman theory (Grahame equation) and estimated the value of the surface potential to be about -50 mV. One problem with this approach is illustrated in Fig. 7, which presents the predictions of the rod (a = 10 Å [1 nm]) and the Gouy-Chapman models for a membrane with a surface potential of about -50 mV bathed in a 0.1 M monovalent salt solution. The rod model predicts that the surface concentration of charged sites on the divalent cation will be enhanced by only a factor of 10 relative to the bulk concentration; the Gouy-Chapman model predicts that the surface concentration will be enhanced by a factor of 40. We conclude that the entropic repulsion of the large cation may have caused a serious error in the previous estimates of the surface potential.

Three additional problems arise in the application of any simple theory to the interaction of these large divalent cations with membranes: the orientation of the binding site on the receptor, its distance from the bilayer framework of the membrane, and the location of the charges responsible for the potential at the binding site are all unknown. As procedures for the reconstitution of purified acetylcholine receptors and sodium channels into bilayer membranes of defined charge become established (25), it should be possible to assess experimentally the importance of each of the above factors.

APPENDIX

Rod Model

Consider a line drawn from charge A to charge B. As illustrated in Fig. 8, the angle this line makes with the normal to the surface is θ. The mean number density of A at a distance x from the surface, $\rho_A(x)$, is the product of the number density of A in the bulk aqueous phase, ρ_A, and the probability that the charge A will be at a distance x from the surface

$$\rho_A(x) = \rho_A \frac{\int_0^{2\pi} d\phi \int_0^{\min[\pi, \cos^{-1}(-x/a)]} d\theta \sin\theta\, g(x + 0.5a\cos\theta, \theta)}{\int_0^{2\pi} d\phi \int_0^{\pi} d\theta \sin\theta}, \quad \text{(A1)}$$

where $g(r,\theta)$ is the probability of finding a molecule D with its center a distance r from the interface making an angle θ with the normal, and $\cos^{-1}(-x/a)$ is the maximum angle θ can obtain if $x < a$ (Fig. 8) because we assume that the ions are confined to the aqueous phase.

The quantity $g(r,\theta)$ is related to the potential of the mean force of the molecule, $W(r,\theta)$, by the equation

$$-\beta W(r,\theta) = \ln[g(r,\theta)]. \quad \text{(A2)}$$

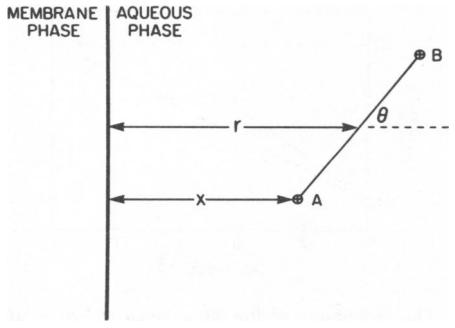

FIGURE 8 Diagram of the divalent cation, of length a, with its center a distance r from the interface. The end A is a distance x from the interface and the line drawn from charge A to charge B makes an angle of θ with the normal to the surface.

In Gouy-Chapman theory the potential of mean force of a point ion at r is replaced by the mean electrostatic potential at r. In a similar way, we write the potential of mean force of molecule D as the sum of the mean electrostatic potentials at each charged site of the molecule

$$-\beta W(r,\theta) = -\beta e\psi(r - 0.5a\cos\theta) - \beta e\psi(r + 0.5a\cos\theta). \quad \text{(A3)}$$

Eq. A3 can be regarded as a one-particle analogue of the interaction site models of molecular fluids (26). Writing $x = r - 0.5a\cos\theta$ (Fig. 8) and $z = x + a\cos\theta$ we obtain

$$g(r,\theta) = \exp[-\beta e\psi(x)]\exp[-\beta e\psi(z)], r > x/2 \quad \text{(A4)}$$

and $g(r,\theta) = 0, r < x/2$ (i.e., $\cos\theta > -x/a$).

Inserting Eq. A4 into Eq. A1 and recalling that $\rho_A = \rho_D$, where ρ_D is the mean number density of divalent cations in the bulk aqueous phase, we obtain Eq. A5, which is identical to Eq. 10 in the body of the text

$$\rho_A(x) = \rho_D\{\exp[-\beta e\psi(x)]\}\{[1/(2a)]\int_{\max[0,x-a]}^{x+a} dz\,\exp[-\beta e\psi(z)]\}. \quad \text{(A5)}$$

Eq. A5 can be derived in a different way. The quantity $\rho_A(x)/\rho_D$ is the normalized probability of finding a given end of the molecule a distance x from the membrane, $\exp[-\beta e\psi(x)]$, weighted by the configurations of the other end of the molecule. This weighting is given by the spatial average of the probability the other end of the molecule is at z, which is $\exp[-\beta e\psi(z)]$. The spatial average is easily calculated by considering a cylindrical coordinate system with its axis perpendicular to the membrane. An infinitesimal unit of area, dA, on a sphere of radius a is $dA = 2\pi a(\sin\theta)a\,d\theta = 2\pi a^2\,d(\cos\theta) = 2\pi a\,dz$. If the integration over the surface of a sphere of radius a with its center a distance x from the membrane is subject to the restriction that the other end of the molecule cannot penetrate the interface, the limits on z become $x + a$ and the maximum value of 0, $x - a$. Eq. A5 follows directly.

String Model

In this case the spatial average of the probability the other end of the molecule is at z is calculated by integrating over the accessible volume in a sphere of radius a located a distance x from the membrane. An infinitesimal unit of volume, dV, in a sphere of radius a is $\pi(a^2 - z^2)\,dz$. If the integration is subject to the restriction that the other end of the molecule cannot penetrate the interface, Eq. 11 follows directly. This treatment is equivalent to assuming that the string joining the two charges does not interact with the surface. That is, no atttempt is made to count the allowed conformational configurations of the string. Alternatively, our string model is equivalent to assuming that the two charges are joined by an infinitely thin, freely telescoping rod of maximum length a. This means that we have accounted for the possible change in the length of the molecule but not the details of the molecular conformations.

S. L. Carnie gratefully acknowledges financial support from the Australian government in the form of a Commonwealth Scientific and Industrial Research Organization (CSIRO) postdoctoral fellowship.

This work was supported by the National Institutes of Health grant PCM 82-00991 to S. McLaughlin.

Received for publication 3 March 1983 and in final form 10 August 1983.

REFERENCES

1. McLaughlin, S., N. Mulrine, T. Gresalfi, G. Vaio, and A. McLaughlin. 1981. Adsorption of divalent cations to bilayer membranes containing phosphatidylserine. *J. Gen. Physiol.* 77:445–473.
2. Lau, A., A. McLaughlin, and S. McLaughlin. 1981. The adsorption of divalent cations to phosphatidylglycerol bilayer membranes. *Biochim. Biophys. Acta.* 645:279–292.
3. Grahame, D. C. 1947. The electrical double layer and the theory of electrocapillarity. *Chem. Rev.* 41:441–501.
4. Verwey, E. J. W., and J. Th. G. Overbeek. 1948. Theory of Stability of Lyophobic Colloids. Elsevier, London.
5. Haydon, D. A. 1964. The electrical double layer and electrokinetic phenomena. *Recent Prog. Surf. Sci.* 1:94–158.
6. Mohilner, D. N. 1966. The electrical double layer. *In* Electroanalytical Chemistry. A Series of Advances. Allen J. Bard, editor. Marcel Dekker, Inc., New York. 1:241–409.
7. Sanfeld, A. 1968. Introduction to the Thermodynamics of Charged and Polarized Layers. John Wiley and Sons, Ltd., London.
8. Barlow, C. A., Jr. 1970. The electrical double layer. *In* Physical Chemistry, An Advanced Treatise. H. Eyring, editor. Academic Press, Inc., New York. 167–246.
9. Sparnaay, M. J. 1972. The Electrical Double Layer. Pergamon Press, Oxford. 415.
10. Aveyard, R., and D. A. Haydon. 1973. An Introduction to the Principles of Surface Chemistry. Cambridge University Press, London. 232.
11. Bockris, J. O'M., and A. K. N. Reddy. 1973. Modern Electrochemistry. Plenum Press, New York. 1432.
12. McLaughlin, S. 1977. Electrostatic potentials at membrane-solution interfaces. *Curr. Top. Membr. Transp.* 9:71–144.
13. Levine, S., and C. W. Outhwaite. 1978. Comparison of theories of the aqueous electric double layer at a charged plane interface. *J. Chem. Soc. Faraday Trans. II.* 74:1670–1689.
14. Alvarez, O., M. Brodwick, R. Latorre, A. McLaughlin, S. McLaughlin, and G. Szabo. 1983. Large divalent cations and the electrostatic potential adjacent to phospholipid bilayer membranes. *Biophys. J.* 44:333–342.
15. Carnie, S. L., D. Y. C. Chan, D. J. Mitchell, and B. W. Ninham. 1981. The structure of electrolytes at charged surfaces: the primitive model. *J. Chem. Phys.* 74:1472–1478.
16. Croxton, T. L., and D. A. McQuarrie. 1979. Numerical solution of the Born-Green-Yvon equation for the restricted primitive model of ionic solutions. *J. Phys. Chem.* 83:1840–1843.
17. Eisenberg, M., T. Gresalfi, T. Riccio, and S. McLaughlin. 1979. Adsorption of monovalent cations to bilayer membranes containing negative phospholipids. *Biochemistry.* 18:5213–5223.
18. McLaughlin, A., W.-K. Eng, G. Vaio, T. Wilson, and S. McLaughlin. 1983. Dimethonium, a divalent cation that exerts only a screening effect on the electrostatic potential adjacent to negatively charged phospholipid bilayer membranes. *J. Membr. Biol.* In press.
19. Torrie, G. M., and J. P. Valleau. 1979. A Monte Carlo study of an electrical double layer. *Chem. Phys. Lett.* 65:343–346.
20. Henderson, R., J. M. Ritchie, and G. R. Strichartz. 1974. Evidence that tetrodotoxin and saxitoxin act at a metal cation binding site in the sodium channels of nerve membrane. *Proc. Natl. Acad. Sci. USA.* 71:3936–3940.
21. Lewis, C. A. 1979. Ion-concentration dependence of the reversal potential and the single channel conductance of ion channels at the frog neuromuscular junction. *J. Physiol. (Lond.).* 286:417–445.
22. Lewis, C. A., and C. F. Stevens. 1979. Mechanism of ion permeation through channels in a postsynaptic membrane. *In* Membrane Transport Processes. C. F. Stevens and R. W. Tsien, editors. Raven Press, New York. 89–103.
23. Adams, D. J., T. M. Dwyer, and B. Hille. 1980. The permeability of

endplate channels to monovalent and divalent metal cations. *J. Gen. Physiol.* 75:493–510.

24. Van der Kloot, W. G., and I. Cohen. 1979. Membrane surface potential changes may alter drug interactions: an example, acetylcholine and curare. *Science (Wash. DC)*. 203:1351–1353.

25. Boheim, G., W. Hanke, F. J. Barrantes, J. Eibl, B. Sakmann, G. Fels, and A. Maelicke. 1981. Agonist-activated ionic channels in acetylcholine receptor reconstituted into planar lipid bilayers. *Proc. Natl. Acad. Sci. USA.* 78:3586–3590.

26. Chandler, D. 1978. Structures of molecular liquids. *Annu. Rev. Phys. Chem.* 29:441–471.